技術論文

Human model on multi-body dynamics simulation of Motorcycle

Motohito Ueki　Akihiro Takayama　Noboru Yabe

当論文は、JSAE 20249005/SAE 2024-32-0005として、SETC2024（Small Powertrains and Energy Systems Technology Conference）にて発表されたものです。

要旨

二輪車の動力学シミュレーションへのライダーモデル追加に関する可能性と課題を検討した。

本研究では、二輪車の動きを運動方程式で再現する10自由度（10-DoF）モデルに加えて、人体の各部位をマスとジョイントで構成した人体モデルを追加した。人体モデルは、腕と肩の角度を制御することで操舵角を操作可能とした。

このモデルの効果を検証するために、固有値解析、定常円旋回、スラローム走行の3つのシミュレーションを実施した。

固有値解析においては、両手をハンドルバーに固定した状態で、ウォブルモードの固有値が根軌跡上で安定側へとシフトすることが確認された。

走行シミュレーションでは、人体モデルの有無による走行影響に加え、人体モデルを介したハンドル操作と直接ハンドルにトルクをかける操作による走行影響が見られた。特にスラローム走行では人体モデルを介したことでの操作遅れが確認された。

これらの結果から、人体モデルがシミュレーションの振動および走行軌跡に影響を及ぼすことが示唆された。

今後はシミュレーションに応じた、人体モデルパラメータの適切な調整が求められる。

Abstract

The possibilities and challenges of adding a rider model to the motorcycle dynamics simulation were investigated for the future planning of a full virtual test.

The human model was added to a multi-body dynamics model that reproduces the equations of motion of a motorcycle, called the 10 degrees of freedom (10-DoF) model. The human model is composed from multiple masses and joints, and the steering angle can be controlled by determining the angle of the arms and shoulder. To study the effect of this model, three distinct simulations were carried out: 'the eigenvalue analysis', 'the steady-state circular test simulation' and 'the slalom running simulation'.

In the eigenvalue analysis, the eigenvalues of the wobble mode shifted to a stable side in the root locus when both hands were fixed on the handlebars.

As a result of the slalom running simulation, the response of the handlebar control through the human model produced a more convex trajectory than a direct control of the steering angle.

For a full virtual test in the future, the human model has some effects to the vibration and trajectory modes of a running simulation. Hence, depending on the purpose of the simulation, the parameters of the human model should be calibrated to fit that purpose.

1 INTRODUCTION

The electrification of vehicles, including motorcycles, is an effective way of achieving a carbon-neutral society. However, an electric unit is a power source with different characteristics from a conventional engine, which also affects the kinematic characteristics of the vehicle. To design motorcycles that take advantage of the characteristics of electric power units, simulation and drivability evaluation technologies that consider the kinematic characteristics are necessary. In addition, motorcycle customers use motorcycles not only for daily use, but also for hobbies such as touring on holidays. Such customers prefer gentle and smooth acceleration and deceleration in their daily use, and in touring situations they prefer vehicles that are powerful yet easy to handle with no unnecessary body movements.

In addition, leaning and turning motorcycles that are lightweight will have a large impact on the body of the vehicle from the human weight transfers and steering maneuvers. Vibrations such as chattering and shift shock are also easily transmitted to the human body, causing unpleasant feelings.

In order to develop products in a short period of time while meeting these complex product requirements, it is necessary to improve the level of simulation technology at the planning stage.

Accordingly, considering prior research, a human model generated with the Biomotion module was incorporated into the motorcycle vehicle motion analysis model on SIMPACK, a multi-body dynamics tool. This allowed us to identify challenges associated with incorporating the human physical model into the analysis.

2 METHOD

In this paper, motorcycle and rider models were prepared for the simulation and assembled to form one model for the calculations. The respective models and modelling methods are presented as follows.

2-1. Motorcycle model

The motorcycle model is based on the 10-DoF equations of motion.

The equations of motion for a motorcycle model with 10-DoF are referenced as follows; the 10-DoF model includes the four degrees of freedom(4-DoF); steering rotation, lateral displacement, vehicle body yaw, and vehicle body roll, that are similar to Sharp's 4-DoF model[1]. The frame consists of a front fork, main frame, and rear swing arm. The degrees of freedom for torsion and lateral bending are represented by lumped stiffness elements. Therefore, six more degrees of freedom are considered in addition to Sharp's 4-DoF model as shown in Fig. 1.

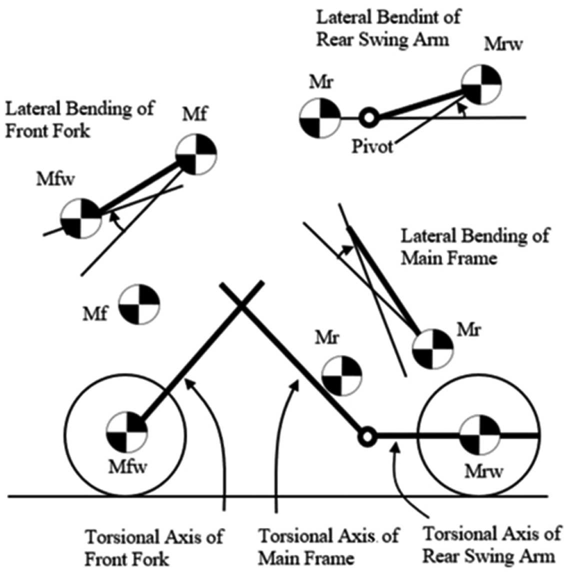

Fig. 1 Geometry of 10-DoF Equations Model "Aoki, et al.; Analysis of the effect of frame rigidity on the straight-line stability of motorcycles, Japan Transactions of the Society of Mechanical Engineers of Japan ©, Vol. 64, No. 625 (1998-9) Paper No.97-1"99"

Aoki et al.[2] reported the effect of frame rigidity on the straight-line stability of motorcycles together with the results of actual motorcycle verification.

Terayama et al.[3] reproduced a 10-DoF model with multi-body dynamics, which is used in this study.

2-2. Rider model

The rider model consists of a human model and a maneuvering controller that was created using the Biomotion module.

2-2-1. Human model

The Biomotion human model is constructed from joints and spring elements connecting several masses. This model rides on the motorcycle model as shown in Fig. 2. The connections are shown in Fig. 3.

Hands-Handle bar: The hands are connected using joints and by aligning the coordinates of the hands with the coordinates of the handlebar position.

Pelvis-Frame: The pelvis is aligned with the seat position coordinates on the frame and connected with a joint.

Legs-Frame: The legs are aligned to the step position coordinates on the frame and are constrained.

The mass and spring characteristics of the human model are shown in Tables 1 and 2. Table 3 shows the characteristics of the connections between the human body parts and the motorcycle.

The parameters in this study used the default values available in Biomotion.

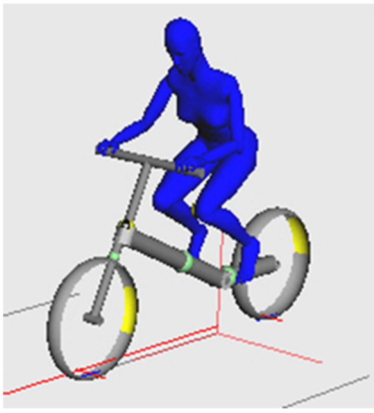

Fig. 2 Rider model and motorcycle model

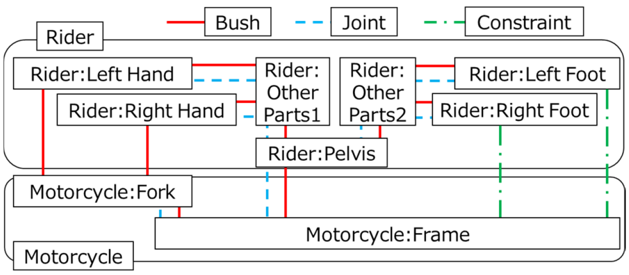

Fig. 3 Relationship between motorcycle model and the human body parts

Table 1 Mass properties of the humanbody parts

Part	Mass [kg]	Ixx [kg m^2]	Iyy [kg m^2]	Izz [kg m^2]
Head	4.814	2.730×10^{-2}	2.452×10^{-2}	2.030×10^{-2}
Neck	1.712	6.387×10^{-3}	6.387×10^{-3}	3.008×10^{-3}
Thorax	15.78[1]	1.760×10^{-1}	7.242×10^{-2}	1.491×10^{-1}
Lumbus	10.60	1.324×10^{-1}	8.468×10^{-2}	5.362×10^{-1}
Upper arm	2.056	1.278×10^{-2}	1.145×10^{-2}	3.966×10^{-3}
Forearm	1.262	6.546×10^{-3}	6.079×10^{-3}	1.299×10^{-3}
Hand	0.486	1.326×10^{-3}	8.840×10^{-4}	5.417×10^{-3}
Pelvis	9.658	6.669×10^{-2}	5.378×10^{-2}	6.060×10^{-2}
Thigh	7.700	2.027×10^{-1}	2.027×10^{-1}	4.260×10^{-2}
Shank	3.215	3.883×10^{-2}	3.738×10^{-2}	6.562×10^{-3}
Foot	0.999	4.444×10^{-3}	2.346×10^{-2}	1.483×10^{-2}

Table 2 Spring constants and damping coefficients between the human body parts

Part	Spring constant [Nm/deg]	Damping coefficient [Nms/deg]
Head-Neck	7.058	4.458×10^{-1}
Neck-Thorax	9.849	6.220×10^{-1}
Thorax-Lumbus	34.47	2.176
Lumbus-Pelvis	47.60	3.007
Upper arm-Thorax	6.566	4.147×10^{-1}
Forearm-Upper arm	2.299	1.451×10^{-1}
Hand-Forearm	2.627	1.659×10^{-1}
Thigh-Pelvis	5.238	3.318×10^{-1}
Shank-Thigh	3.939	2.489×10^{-1}
Foot-Shank	3.283	2.074×10^{-1}

Table 3 Spring constants and damping coefficients between the human model and the motorcycle

Human model-motorcycle	Spring constant		Damping coefficient	
	Translation [N/m]	Rotation [Nm/deg]	Translation [Ns/m]	Rotation [Nms/deg]
Handlebar-Hand	6.0×10^{4}	5.236	1.0×10^{2}	1.745×10^{-1}
Frame-Pelvis	3.0×10^{4}	8.727	3.0×10^{3}	1.745×10^{-1}

2-2-2. Maneuvering controller

The maneuvering controller uses part of the Biomotion module. It is equipped with acceleration and deceleration controls in the longitudinal speed and the lateral direction, which are controlled by steering angle. To assess the impact of the human model, two distinct control modes were prepared, the SAD mode and the HC mode.

SAD (Single Axis Direct): To match the target steering angle, the steering torque is controlled by direct input to the steering axis.

HC (Handlebars Control): To match the target steering angle, the steering torque is input to the handlebar through the human body elements, which controls the angle of the forearm and the upper arm.

Both control modes use look-ahead models as shown in Fig. 4. This model checks the trajectory and steers the motorcycle towards the target trajectory in both the steady state circular test simulation and in the slalom running simulation. The rider model looks at the estimated position after 1.1 sec from the present time. In this study, this parameter was tuned to avoid falling, but it has not been validated by any test or verification.

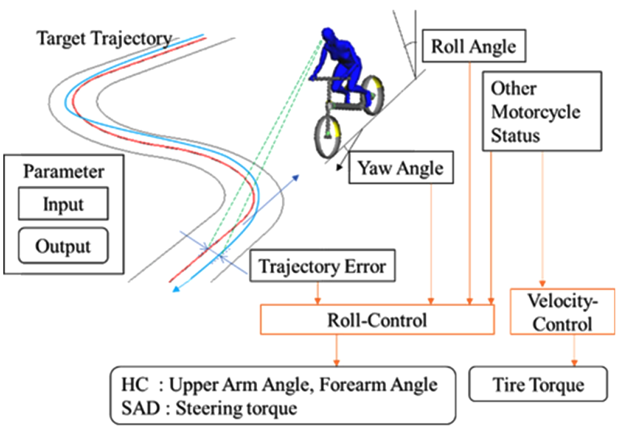

Fig. 4 Maneuvering image

The 'Trajectory Error' is the distance QP, which is the distance in the normal direction between point P, which is a point extended from the current position by the distance of the look ahead on the 'target trajectory', and point Q, which is the extension point of the 'direction of motorcycle travel', as shown in Fig. 5. The steering angle of SAD or the angles of human parts of HC are calculated by each PID controller. As long as the human body model is represented by a spring mass model, some of the response delay will be included in the result of maneuvering model or in the elements of the human body parts.

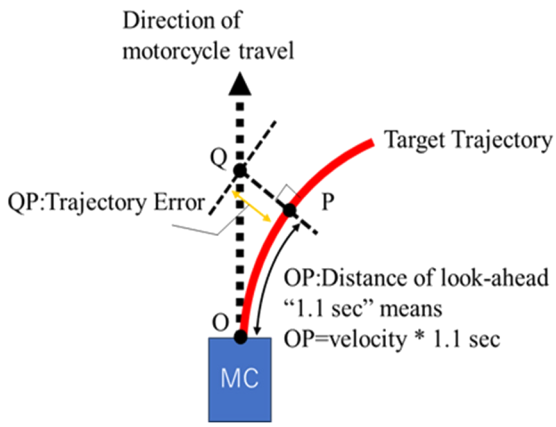

Fig. 5 Trajectory error image

2-3. Analysis and Simulation

To study the influence of the human model and the maneuvering model to the motorcycle behavior, the following is the list of analyses or simulations used.

Table 4 List of analyses and simulations

Target	State	Analysis/Simulation
Static characteristics (Eigenvalue Analysis)	Static	Frequency response
Dynamic characteristics (Driving Simulation)	Steady	Steady state circular test
	Transient	Slalom running

To study the influence of maneuvering and dynamic characteristics, the driving simulation was provided with two types of maneuvering controllers, the SAD mode and the HC mode in Biomotion.

The MF-Tire was used as the tire model for all simulations.

2-3-1. Eigenvalue Analysis

To study how a rider influences the motorcycle vibration characteristics, two motorcycle models were prepared; one with a rider and the other without a rider. The wobble and weave modes are typical motorcycle vibration modes with frequencies under 10 Hz. In the past study, we know that the handlebar operation produced different results from the no rider model. Therefore, the frequency analyses were conducted on the motorcycle-only model and the combined rider model.

・Handle-free: The rider's hands are not connected to the handlebars.
・Fixed handlebar: The handlebars are connected to the hands of the human model.
・STD 10-DoF: The rider was represented by a mass property fixed to the motorcycle mass property.

2-3-2. Steady state circular test

The radius of the circle was set to 150 m, and motorcycle speed was simulated from 80 km/h to 120 km/h in 10 km/h increments as shown in Table 6. Fig. 6 shows one of the driving simulation cases.

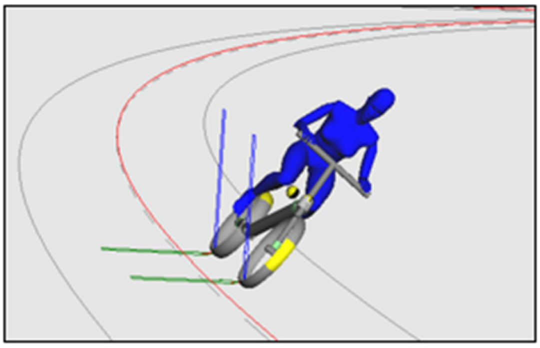

Fig. 6 Driving simulation representing the steady state circular test

To assess the impact of the human model, the two distinct control modes, the SAD mode and the HC mode were differentiated, as detailed in chapter 2-2-2.

2-3-3. Slalom running

The slalom test was simulated to study a maneuver controller in a transient state. Fig. 7 shows one of the driving simulation cases. Three rider models were compared as shown in Table 5. The slalom course was defined as sinusoidal, and the amplitude was gradually increased until it reached 200 m. From 200 m to 500 m, the amplitude takes a constant value is shown in Table 6.

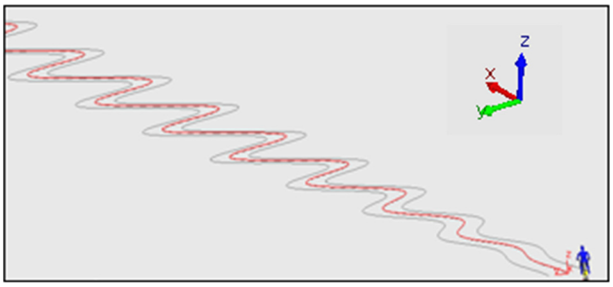

Fig. 7 Driving trajectory in the slalom running simulation

Table 5 Rider models for the slalom running simulation

	Human model	Maneuvering controller
Human model with SAD	Human (Biomotion)	SAD
Human model with HC		HC
STD 10-DoF with SAD	Rigid (STD 10-DoF)	SAD

Table 6 Driving simulation conditions

	Steady state circular test	Slalom Running
Driving course	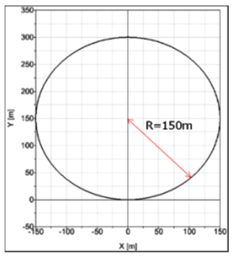	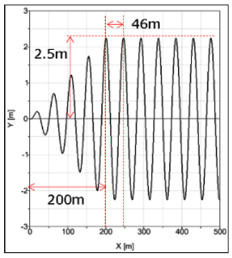
Motorcycle speed	80~120km/h (in 10km/h increments)	40km/h

3 RESULT

3-1. Eigenvalue Analysis

The wobble and weave modes in each condition are shown in the root locus plot as shown in Fig. 8.

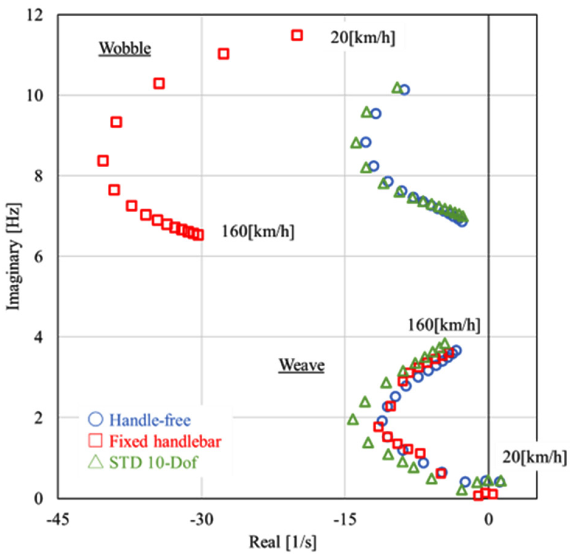

Fig. 8 Root-locus plot for the eigenvalue analysis

The locus of the wobble mode shifted to the stable side in the 'Fixed handlebar' model compared to the 'Handle-free' model. When a human body was attached to the handlebar in the 'Fixed handlebar' model, the steering angle movement was suppressed by a spring and damper system as represented by the human body parts. In the previous paper [4], the force of a handle push increased the number of wobble vibrations and moved the locus to the stable side.

However, in this paper, the results were calculated using the default parameters of Biomotion. These parameters need to be validated by test measurements for a more accurate analysis result.

3-2. Steady state circular test

Under the steady state conditions, the criteria for the orientation of the angle between the forearm and the upper arm are shown in Fig. 9. The direction of each arrow shows the axis of rotation.

The simulation results for the steering angle, roll angle, steering torque, front/rear tire lateral forces and forearm/upper arm angle at different motorcycle speeds are shown in Fig. 10. The legend in Fig. 10 indicates the maneuvering methods (SAD, HC).

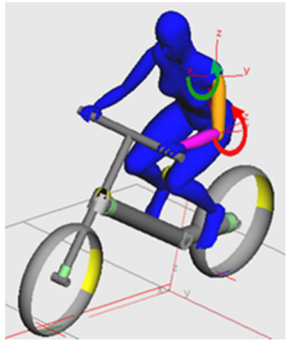

Fig. 9 Reference axes for the Forearm/Upper arm angles on the human model

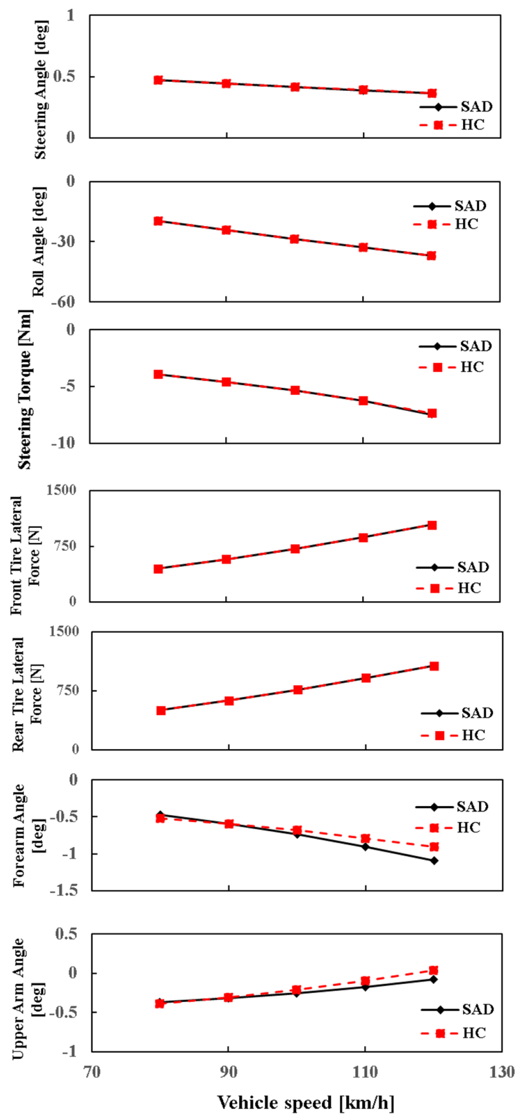

Fig. 10 Results of the 'Steady state circular test' simulation

3-3. Slalom Running

The results of the travel trajectory as shown in Fig. 11 show that the motorcycle follows the runway with a larger amplitude in the Y direction than the target trajectory. It was found that sinusoidal running in constant amplitude can itself be performed in the region beyond 200 m of the X-axis distance, although it has moved away from the target. In addition, the trajectory did not shift even if the control method was changed in the same way as for the steady state circular test. Since, it was found that the trajectory was almost the same even if there was a difference in the presence or absence of a human model.

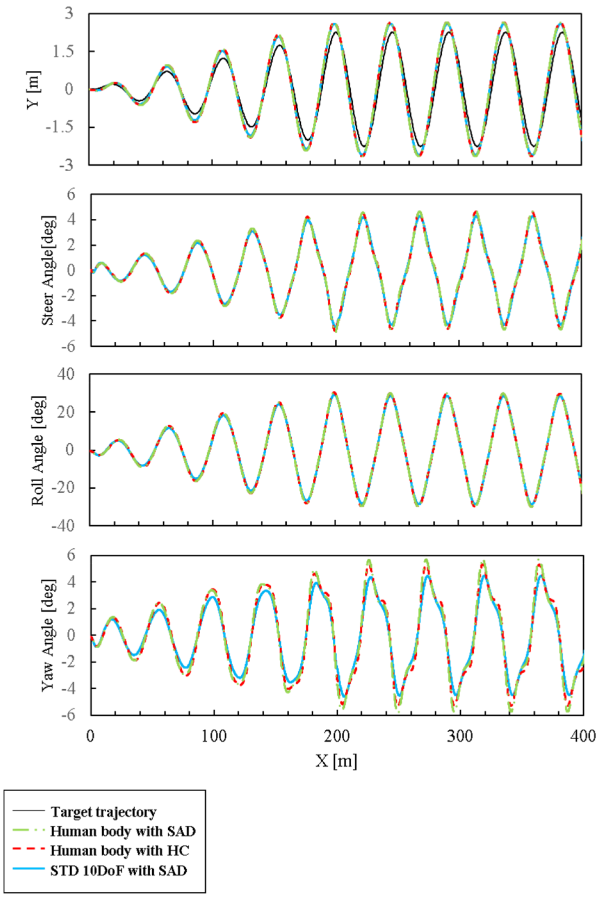

Fig. 11 Results of the 'Slalom running' simulation in 40 km/h

The trajectory of the enlarged chart is shown in Fig. 12, which indicates that the 'STD 10-DoF with SAD' was tracing in the closest proximity to the target trajectory because this had been directly connected to the controller without any delayed movement and effect from behavior of human parts. The trajectories of the 'Human body with HC' and 'Human body with SAD' models exhibited slightly more convex shapes, with the former turning later than the latter.

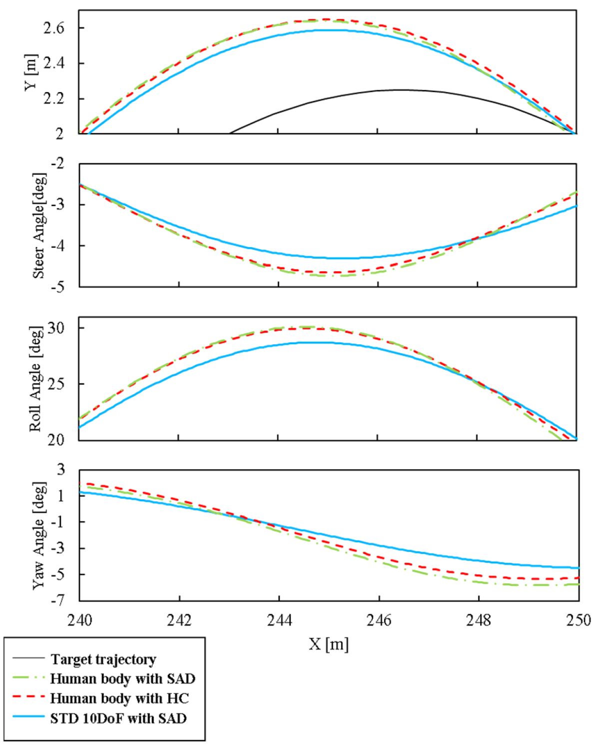

Fig. 12 Enlarged chart of the 'Slalom running' simulation from 240 m to 250 m

Due to the delay in control through the arms, the steering angle of the 'Human body with HC' was smaller than that of the 'Human body with SAD' at 242-246 m as shown in Fig. 11. Also, the roll angle in HC mode was smaller than in SAD mode at 244-248 m due to the delay in the maneuver.

It was explained in chapter 2.2.2 that 'Human body with SAD' determines the angles of the Forearm and Upper arm by directly controlling the steer angle with respect to the target steer angle, whereas 'Human body with HC' controls the steer angle by adjusting the Forearm and Upper arm to the target steer angle and operating the steering. These delays were caused by this control difference.

4 CONCLUSION

By using Biomotion on SIMPACK, the human model could be used in the motorcycle multibody dynamics simulation.

The human model affected the eigenvalues of the wobble mode in the same way as in the previous paper. In the slalom running, the human model caused a delay in the steering angle control and the trajectory convex shape.

In this paper, all parameters of the human parts were set to their default values. However, the results indicated that, depending on the purpose, the validation of a spring constant and a damping coefficient is crucial for an accurate simulation. Therefore, one solution is to use the machine learning method[5] to calibrate these parameters in the short term.

REFERENCES

[1] Sharp, R. S. : The Stability and Control of Motorcycles, Journal of Mechanical Engineering Science, Vol. 13, No. 5, 316-329, 1971.

[2] Aoki, A., Nishimi, T., Okayama, T., Katayama, T.: Analysis of the effect of frame rigidity on the straight-line stability of motorcycles, Transactions of the Japan Society of Japan Mechanical Engineers (C), Vol. 64, No. 625 (1998-9), Paper No., 97-1799.

[3] Terayama, T., Yamaguchi, S., Kitagawa, H., Yabe, N., Reproducing the Motorcycle Equation of Motion with Lumped Stiffness on Multi-Body Dynamics Model, SAE Technical Paper 2023-01-1828, 2023.

[4] Kageyama, I., Kogo, A.: Human factors in the steering system of two wheeled vehicles, JSME 28 (240), 1233-1239, 1985.

[5] Mitsuhashi, Y., Takeshita, H., Momiyama, Y., Yabe, N., Study on Motorcycle Rider Model using Reinforcement Learning—Basic Research to Represent the Behavior according to the Rider Proficiency—, JSAE Technical Paper, 559-564, Vol. 55, No. 3, 2024.

■著者

植木 幹人
Motohito Ueki
技術・研究本部
デジタル開発統括部
MBSE 推進部

高山 照浩
Akihiro Takayama
技術・研究本部
デジタル開発統括部
MBSE 推進部

矢部 昇
Noboru Yabe
技術研究本部
デジタル開発統括部
MBSE 推進部